

Proceedings

# Modification of SnO<sub>2</sub> Nanowires with TeO<sub>2</sub> Branches and Their Enhanced Gas Sensing †

Myung Sik Choi <sup>1</sup>, Jae Hoon Bang <sup>1</sup>, Ali Mirzaei <sup>2</sup>, Hyoun Woo Kim <sup>1,2,\*</sup> and Sang Sub Kim <sup>3,\*</sup>

<sup>1</sup> Department of Materials Science and Engineering, Hanyang University, Seoul 133-791, Korea; choigocms@gmail.com (M.S.C.); ps04407@naver.com (J.H.B.)

<sup>2</sup> The Research Institute of Industrial Science, Hanyang University, Seoul 133-791, Korea; alisonmirzaee@yahoo.com

<sup>3</sup> Department of Materials Science and Engineering, Inha University, Incheon 402-751, Korea

\* Correspondence: hyounwoo@hanyang.ac.kr (H.W.K.); sangsub@inha.ac.kr (S.S.K.);  
Tel.: +82-10-8428-0883 (H.W.K.); +82-10-9885-6182 (S.S.K.)

† Presented at the Eurosensors 2017 Conference, Paris, France, 3–6 September 2017.

Published: 17 August 2017

**Abstract:** We prepared a highly sensitive and selective NO<sub>2</sub> sensor, based on the TeO<sub>2</sub> branched SnO<sub>2</sub> nanowires (NWs), in terms of vapor-liquid-solid method, with subsequent growing of branches on the stems of SnO<sub>2</sub> NWs. Fabricated sensors showed a high response higher than 10 to 10 ppm of NO<sub>2</sub> gas at 100 °C. We investigated the associated sensing mechanisms, with respect to the enhancement of sensing behaviors by the addition of TeO<sub>2</sub> branches. Based on the results obtained in this work, we believe that the present sensor with an efficient fabrication technique, and high sensitivity and selectivity can be used for detection of NO<sub>2</sub> gas in real applications.

**Keywords:** SnO<sub>2</sub> nanowires; TeO<sub>2</sub> branches; gas sensing

## 1. Introduction

Nanostructures are attractive and important structure in gas sensor criteria, because they can be manipulated easily and gas sensing properties are different depending on their morphologies [1]. Among that one-dimensional nanowires have been experimented as attractive materials to chemical gas sensors. Especially, the branched nanowires are tested for several reasons [2]. First, they have strength of 1-D nanowires. They have a linear path of charge transportation, which reduces carrier diffusion lengths and improves electron transportation. Second, branched nanowires have large surface area than 1-D nanowires, which enables many reactants to react on the surface of sensing materials. Accordingly, it enhances gas sensing properties such as sensitivity and selectivity.

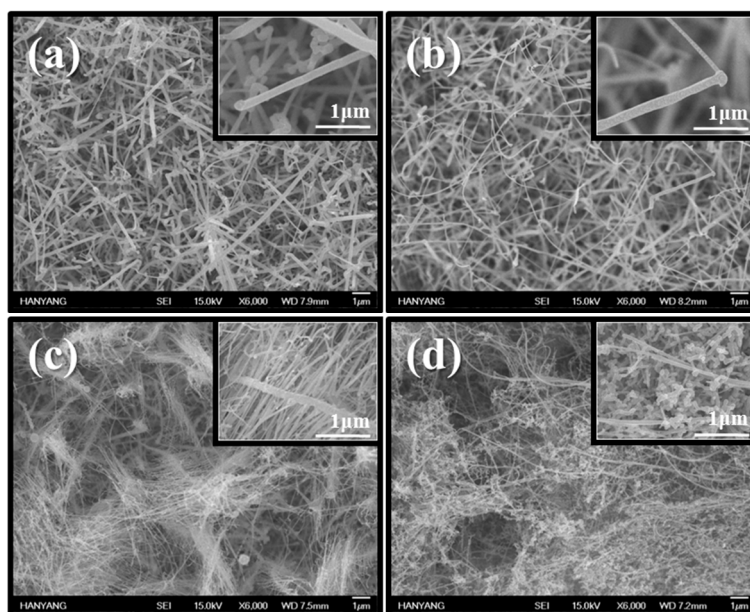
## 2. Experimental

The fabrication procedures of TeO<sub>2</sub> branched SnO<sub>2</sub> nanowires are as follows. First, SnO<sub>2</sub> nanowires were fabricated by thermal evaporation of Sn powder. Sn powder (purity: 99.9%, Sigma-Aldrich) was used as the source material. The substrate was set to 900 °C for 1hr to heat 3 nm-Au coated Si substrates. A mixture of O<sub>2</sub> and Ar gases (O<sub>2</sub>: 3%; Ar: 97%) was set at a fixed 2 Torr pressure. Then, TeO<sub>2</sub> branches were grown onto the surface of SnO<sub>2</sub> nanowires with the same VLS procedure only with the different temperature of 370 °C. For the sensing experiments, Ti/Au electrodes were sputtered on specimens with a turbo sputter coater (Emitech K575X, Emitech Ltd., Ashford, Kent, UK) and as-fabricated sensors were placed in a horizontal quartz tube furnace for gas sensing test. Through mass flow controllers, concentrations of target gases were manipulated by changing the mixing ratio of the target gas and dry air, with a total flow rate of 500 sccm. The resistances of sensors in the presence of air (R<sub>a</sub>) and target gas (R<sub>g</sub>) were measured and the sensor

response for oxidative gas ( $\text{NO}_2$ ) was calculated as  $R = R_g/R_a$ , and for reducing gases was calculated as  $R = R_a/R_g$ .

### 3. Results and Discussion

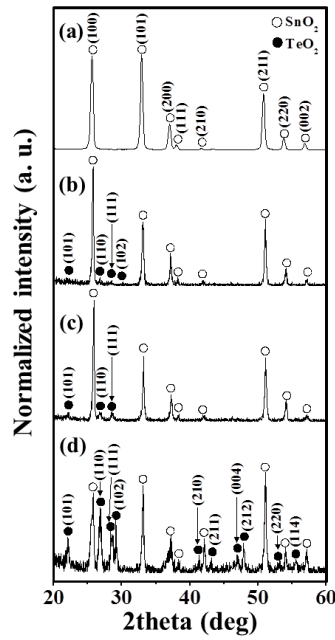
Figure 1a is SEM images of  $\text{SnO}_2$  nanowires and Figure 1b–d is SEM images of  $\text{TeO}_2$  branched  $\text{SnO}_2$  nanowires with annealing temperature at 320, 370 and 420 °C. Branches were grown randomly onto the surface of  $\text{SnO}_2$  nanowires. Figure 2a shows an XRD pattern of pristine  $\text{SnO}_2$  nanowires, exhibiting reflection peaks that can be indexed to the tetragonal rutile  $\text{SnO}_2$  phase (JCPDS card: No. 41-1445). Figure 2b–d show XRD pattern of  $\text{SnO}_2$  nanowires with orthorhombic  $\text{TeO}_2$  (JCPDS card: No. 52-1005) branches with different temperature. Figure 3a shows low magnification TEM images of  $\text{TeO}_2$  branched  $\text{SnO}_2$  nanowires. Figure 3b,c shows SAED pattern and Lattice-resolved TEM image of  $\text{TeO}_2$  branched  $\text{SnO}_2$  nanowires.



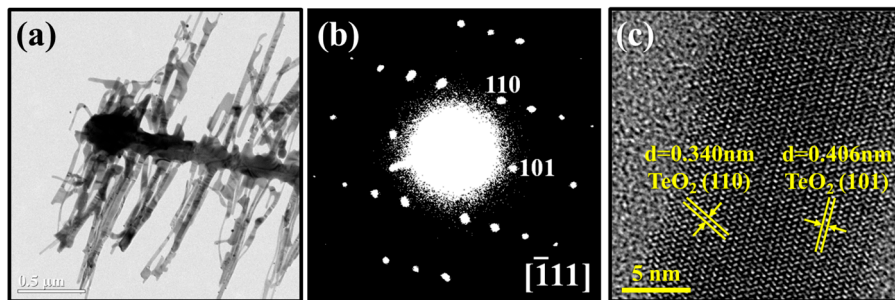
**Figure 1.** SEM images of (a)  $\text{SnO}_2$  nanowires,  $\text{TeO}_2$  branched  $\text{SnO}_2$  nanowires with annealed at (b) 320 °C, (c) 370 °C, and (d) 420 °C.

Figure 4 shows the sensing performances of pristine  $\text{SnO}_2$  nanowires and  $\text{TeO}_2$  branched  $\text{SnO}_2$  nanowires. Figure 4a shows the sensor responses, revealing that the responses of branched  $\text{SnO}_2$  nanowires are higher than those of pristine  $\text{SnO}_2$  nanowires at temperatures in the range of 25–150 °C. Figure 4b shows the response times, indicating that the response time tends to decrease with increasing the temperature and that the response time of  $\text{TeO}_2$  branched  $\text{SnO}_2$  nanowires is shorter than that of pristine  $\text{SnO}_2$  nanowires. Figure 4c shows the recovery times, exhibiting that the response time also tends to decrease with increasing the temperature and that the response time of branched  $\text{SnO}_2$  nanowires is shorter than that of pristine  $\text{SnO}_2$  nanowires.

We investigated the associated sensing mechanisms, in regard to the enhancement of sensing performances by the incorporation  $\text{TeO}_2$  branches. It is revealed that not only the  $\text{TeO}_2$  branches themselves but also the heterojunctions of  $\text{SnO}_2/\text{TeO}_2$  play a crucial role in enhancing the sensing behaviors.



**Figure 2.** XRD images of (a) SnO<sub>2</sub> nanowires, TeO<sub>2</sub> branched SnO<sub>2</sub> nanowires with annealed at (b) 320 °C, (c) 370 °C, and (d) 420 °C.



**Figure 3.** TEM analysis of a TeO<sub>2</sub> branched SnO<sub>2</sub> nanowires with annealing temperature of 370 °C. (a) Low-magnification TEM image, (b) SAED pattern, and (c) Lattice-resolved TEM image.

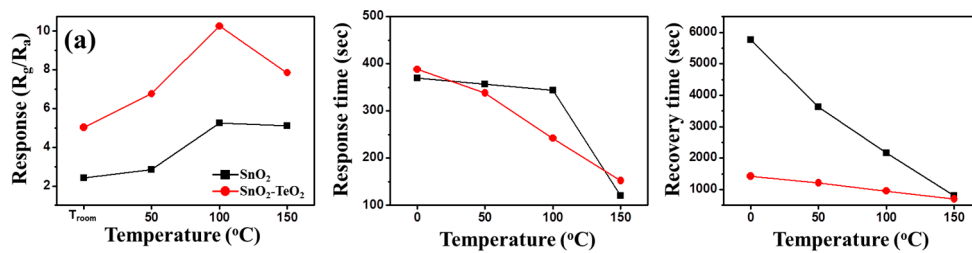


**Figure 4.** (a) Response curve of SnO<sub>2</sub> nanowires (Black) and TeO<sub>2</sub> branched SnO<sub>2</sub> nanowires (Red), (b) Response times and (c) Recovery times of SnO<sub>2</sub> nanowires and TeO<sub>2</sub> branched SnO<sub>2</sub> nanowires

#### 4. Conclusions

In this work, a highly sensitive and selective NO<sub>2</sub> sensor, based on the TeO<sub>2</sub> branched SnO<sub>2</sub> nanowires (NWs) were synthesized by an efficient route. Fabricated sensor showed a high response to 10 ppm of NO<sub>2</sub> gas at optimal temperature of 100 °C, demonstrating an excellent selectivity of sensor towards NO<sub>2</sub> gas. The superior sensing properties of branched NWs sensor relative to the pristine sensor were mainly attributed to the branch-induced high surface area of sensor and formation of homo- and heterojunctions between SnO<sub>2</sub> and TeO<sub>2</sub>.

**Acknowledgments:** This research was supported by Basic Science Research Program through the National Research Foundation of Korea (NRF) funded by the Ministry of Education (2016R1A6A1A03013422).

**Conflicts of Interest:** The authors declare no conflicts of interest

## References

1. Sarkar, A.; Kanakamedala, K.; Jagadish, N.N.; Jordan, A.; Das, S.; Siraj, N.; Warner, I.M.; Daniels-Race, T. Electro-optical characterization of cyanine-based GUMBOS and nanoGUMBOS. *Electron. Mater. Lett.* **2014**, *10*, 879–885.
2. Wan, Q.; Huang, J.; Xie, Z.; Wang, T.H.; Dattoli, E.N.; Lu, W. Branched SnO<sub>2</sub> nanowires on metallic nanowire backbones for ethanol sensors application. *Appl. Phys. Lett.* **2008**, *92*, 102101.



© 2017 by the authors. Licensee MDPI, Basel, Switzerland. This article is an open access article distributed under the terms and conditions of the Creative Commons Attribution (CC BY) license (<http://creativecommons.org/licenses/by/4.0/>).